REPORT DOCUMENTATION PAGE

The public reporting burden for this collection of information is estimated to average 1 hour per response, including the time for reviewing instructions, searching existing data sources, gathering and maintaining the data needed, and completing and reviewing the collection of information. Send comments regarding this burden estimate or any other aspect of this collection of information, including suggestions for reducing the burden, to Department of Defense, Washington Headquarters Services, Directorate for Information Operations and Reports (0704-0188). 1215 Jefferson Davis Highway, Suite 1204, Arlington, VA 22202-4302. Respondents should be award that notwithstanding any other provision of law, no person shall be subject to any penalty for failing to comply with a collection of information if it does not display a currently valid OMB control number.
PLEASE DO NOT RETURN YOUR FORM TO THE ABOVE ADDRESS.

1. REPORT DATE (DD-MM-YYYY)	2. REPORT TYPE	3. DATES COVERED (From - To)
11-DEC-2003	Conference Proceedings, (refereed)	

4. TITLE AND SUBTITLE	5a. CONTRACT NUMBER
Multi-Robot Position Tracking	5b. GRANT NUMBER
	5c. PROGRAM ELEMENT NUMBER

6. AUTHOR(S)	5d. PROJECT NUMBER
MARVIN W ROE BRIAN S BOURGEOIS PATRICK MCDOWELL	5e. TASK NUMBER
	5f. WORK UNIT NUMBER
	74-6636-04

7. PERFORMING ORGANIZATION NAME(S) AND ADDRESS(ES)	8. REPORTING ORGANIZATION REPORT NUMBER
Naval Research Laboratory Marine Geoscience Division Stennis Space Center, MS 39529-5004	NRL/PP/7440--03-1032

9. SPONSORING/MONITORING AGENCY NAME(S) AND ADDRESS(ES)	10. SPONSOR/MONITOR'S ACRONYM(S)
Office of Naval Research 800 North Quincy Street Arlington, VA 22217	ONR
	11. SPONSOR/MONITOR'S REPORT NUMBER(S)

12. DISTRIBUTION/AVAILABILITY STATEMENT

Approved for public release, distribution is unlimited

13. SUPPLEMENTARY NOTES

14. ABSTRACT

Accurate navigation is just one of the many challenges for successfully coordinating multiple robot interaction. It is especially important when trying to quantify the success of new techniques being developed to achieve coordinated formation maneuvering. This paper presents the experimental procedures followed while determining robot navigation error along with an evaluation of the resultant measurements. An inexpensive, easily configurable, camera system is presented that shows the potential to provide accurate position information. Along with a description of the system configuration, test procedures and test data are presented and evaluated. Finally, a comparison of the robot navigation error to that of the proposed camera system is presented.

15. SUBJECT TERMS

navigation, multiple robot interaction, coordinated formation maneuvering

16. SECURITY CLASSIFICATION OF:			17. LIMITATION OF ABSTRACT	18. NUMBER OF PAGES	19a NAME OF RESPONSIBLE PERSON
a. REPORT	b. ABSTRACT	c. THIS PAGE			Marvin Roe
Unclassified	Unclassified	Unclassified	Unlimited	5	19b. TELEPHONE NUMBER (Include area code) 228-688-4937

Standard Form 298 (Rev. 8/98)

Multi-robot Position Tracking

(Full Draft)

Marvin Roe	Dr. Brian Bourgeois	Patrick McDowell
Naval Research Laboratory	Naval Research Laboratory	Naval Research Laboratory
Stennis Space Center, MS	Stennis Space Center, MS	Stennis Space Center, MS
39529-5004, USA	39529-5004, USA	39529-5004, USA
228.688.3947	228.688.5321	228.688.4823
mroe@nrlssc.navy.mil	bsb@nrlssc.navy.mil	pmcdowell@nrlssc.navy.mil

ABSTRACT

Accurate navigation is just one of the many challenges for successfully coordinating multiple robot interaction. It is especially important when trying to quantify the success of new techniques being developed to achieve coordinated formation maneuvering. This paper presents the experimental procedures followed while determining robot navigation error along with an evaluation of the resultant measurements. An inexpensive, easily configurable, camera system is presented that shows the potential to provide accurate position information. Along with a description of the system configuration, test procedures and test data are presented and evaluated. Finally, a comparison of the robot navigation error to that of the proposed camera system is presented.

Categories and Subject Descriptors
Autonomy, Underwater Vessels, Multi-Agent Systems, Simulation

General Terms
Performance, Design, Reliability, Experimentation, Theory, Standardization

Keywords
Unmanned Underwater Vessel, Autonomous, Navigation, Position, Timing, Communication, Dead Reckoning

1. INTRODUCTION

Interest in the use of multiple unmanned underwater vehicles (UUVs) for military and commercial purposes is growing because of the potential benefits to underwater operations such as searching, inspection, and surveying. NRL researchers are developing control, communications and positioning methods to enable the use of multiple UUV formations. In the undersea environment traditional methods of communication and navigation (radio and GPS) are ineffective because of the properties of seawater, making control of the UUVs a difficult proposition.

Because inertial based vessel positioning systems typically yield position error growth on the order of 1% of the distance traveled [1] they are not adequate for formation maneuvering. The only viable alternative underwater for communications and positioning is acoustics but these systems yield fairly short ranges and very low bandwidths [2]. A promising approach is vessel relative positioning and navigation using combined communication/position acoustic systems. Formation maneuvering based on inter-vessel positioning and navigation has distinct advantages in that it can reduce or eliminate the requirement for pre-deployed positioning systems and it can be used to increase the sensor footprint in searching and surveying tasks.

To date with this work, systems and control algorithms have been developed that allow 3 mobile robots to follow each other using acoustic signaling in a laboratory. An example of this is shown in Figure 1. While qualitative results have been demonstrated, quantifiable results require an accurate local area positioning system in the lab and that is the focus of this paper. The robots determine their position and heading relative to their startup position using dead reckoning based on wheel counts. While they are equipped with a magnetic compass, the metal structures in the lab create local variations in the magnetic field as great as 60°, rendering them unusable. In this paper we present the method and results of testing of the dead reckoning capability of the robots. We further present a preliminary design for a camera based positioning system and show preliminary results of camera tests.
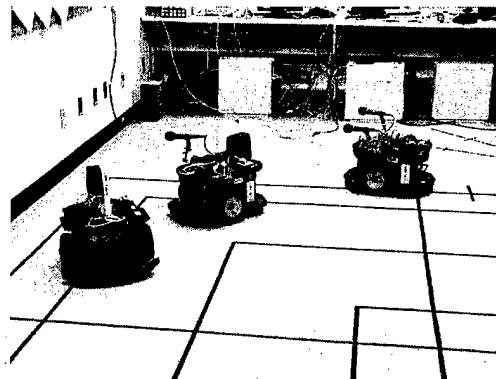

Figure 1. This figure shows a three robot following test. The lead robot on the left is being operated manually while the 2nd and 3rd robots are using their microphones to track the robots in front of them.

2. ROBOT DEAD RECKONING

In order to present justifiable and repeatable experimental parameters that support the quantification of the relative navigation research, the accuracy of sensor feedback from the robots and equipment must be known. This section presents the findings of experiments done to determine the cumulative error observed during dead reckoning waypoint following by the robots. The key characteristics to be determined are the amount, nature, and variance of the error.

The lab is equipped with a control center that consists of a set of 3 pc's running Windows 2000 that control ActivMedia robots via wireless Ethernet. The robots utilize high–resolution optical quadrature shaft encoders for position and speed sensing as discussed in [3]. The software used to operate the robots consists of a client/server configuration that was developed using a combination of LabVIEW, omniOrb CORBA, C++, and the robot's supplied API libraries. LabVIEW provides the GUI, configuration, and execution control and CORBA, C++, and the robot API provide network connectivity and robot operation. The RobotClient program runs on the each of the control center PC's and connects to an instance of the RobotServer running on each of the robots, which are also configured with Windows 2000. The RobotClient GUI provides a view of the sensor feedback on a grid that coincides with a 400 cm by 400 cm grid with the origin in the center on the lab floor so that visual progress of the sensor values and the robot's physical position can be observed at the same time.

Each run of the experiments was conducted with the use of a waypoint following program that guided the robot over a course represented by x, y positions. The waypoint program runs in it's own thread within the RobotServer application and has both it's configuration and execution controlled via the RobotClient. A hit radius of 20 cm was chosen for the robot to determine accomplishment of finding each waypoint. A speed of 100 mm/sec was set along with a max rotational velocity of 30 deg/sec for the robot. Progress to each waypoint was evaluated by comparing the robot's sensed position and heading to the location of the next waypoint. Adjustments to the robot's heading were made, if necessary, followed by a one second sleep interval that separated each update.

Figure 2. Measuring Robot Position

For more accurate physical measurement of robot positions, a combination of square metal rulers, duct tape, and paper clips were used to identify points at the front, rear, left and right of the robot platform. As shown in figure 2, these points were aligned with the ruler to accurately position the robot or to transcribe those points to the floor. Connecting these points provided a cross-hair that could be used to determine both position and heading. This was useful since the center point of the robot is defined as a point in the middle of the axle line.

Due to timing, variances in each path, and the 20 cm hit radius, the robot wasn't expected to stop with the exact same sensor values for every run. Furthermore, since the purpose of this experiment was to determine the error between sensor readings and the robot's actual physical position and heading after traveling some distance, only the final robot position sensor values and physically measured position values are presented.

Three experiment paths were evaluated to obtain navigation error data. The paths consisted of a counterclockwise path, clockwise path, and a straight path. Prior to each experiment, the robot's tires were set to a pressure 32psi to help ensure equal tire diameters. Each experiment path was run 10 times with the robot's sensors being reinitialized for each run.

3. COUNTER-CLOCKWISE AND CLOCKWISE PATH EXPERIMENTS

The counter-clockwise path experiment consisted of a set of waypoints that guided the robot around the grid on the UNCL floor in a square shaped path that had the robot always turning to the left. The series of waypoints began with a starting point of 120, 0 with a heading of 90deg. The rest of the waypoints for the path were as follows: 120, 120; -120, 120; -120, -120; 120, -120. The final waypoint in the series was 120,120 and for each run the robot would stop when its sensor readings were within the 20 cm hit radius value. The counter-clockwise path was approximately 39.6 meters of linear travel and included 1440 degrees of turning to the left. Figure 3 shows a scatter plot of the sensor feedback and measurements of the robot's final position for each of the 10 experiment runs.
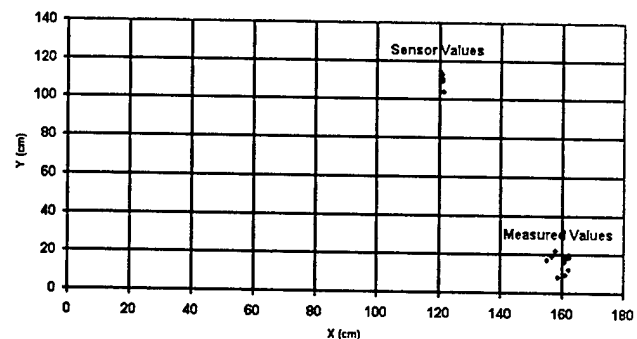

Figure 3. Counter-Clockwise position scatter plot showing the recorded sensor values and measured position values for the experiment.

Figure 4 shows the ranges of sensor headings and measured headings recorded for the robot's stopping points for the ten experiment runs. The mean position error for all runs was 103.3cm with a standard variation of 4.2cm. The mean heading error was 37.1° with a standard deviation of 1.3°. The results of

the clockwise path experiment yielded results of 164.9cm with a standard variation of 3.9cm. The mean heading error was 66.4° with a standard deviation of 3.4°.

4. STRAIGHT PATH EXPERIMENT

The straight path experiment consisted of a set of waypoints that guided the robot along a path directly aimed at a heading of 90 degrees with no turns to the left or right across the grid on the floor that started at 0, -350 and went to the point 0, 450. The path was executed once for each of the 10 experiment runs.
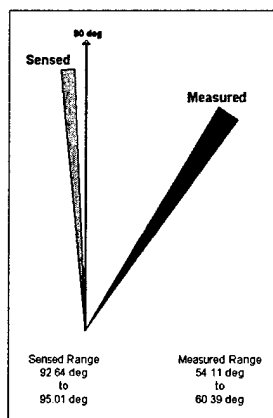

Figure 4. Ranges of experimental results for sensed and measured heading shown to scale for the counter-clockwise path.

The robot would stop when its sensor readings were within the 20 cm hit radius value of the final waypoint. The straight path consisted of approximately 8 meters linear travel and included 0 degrees of change to heading. A scatter plot of the sensor feedback and measurements of the robot's final position for each of the 10 experiment runs is provided in figure 5. The mean position error for all runs was 56.7cm with a standard variation of 4.4cm. The mean heading error was 8.9° with a standard deviation of 0.5°.
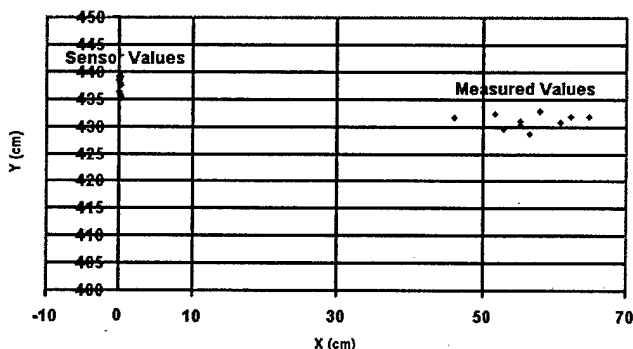

Figure 5. Straight path position scatter plot showing the recorded sensor values and measured position values for the experiment.

We see from these results that the drift in position and heading using dead reckoning is very repeatable, i.e. if the robot follows the same path it will arrive very closely to the same position. The tests reveal that dead reckoning position errors for these robots is

about 2.6% of the distance traveled for the counter-clockwise path, 4.1% for the clockwise path and 7% for the straight path. This error growth rate is typical of unmanned underwater vessels equipped with dead reckoning position systems consisting of a magnetic compass and a Doppler Velocity Log. With this error growth rate, the robots have over a 1m error after only 4 laps around the lab. Consequently an external positioning system is required for extended runs and assessment of multi-robot control approaches.

5. CAMERA SYSTEM DESIGN

The external positioning system proposed will incorporate a Web camera that is easily positioned and configured in the lab or outdoors. For the lab, mounting the camera directly above the lab floor does not provide enough image coverage due to the height of the ceiling. Similar systems have been built for use in RoboCup League competitions but these systems locate the camera directly above the center of the field of play [4]. The use of a wide angle lens would increase the image field of view but introduce computational overhead to compensate for barrel distortion effects due to lens design as discussed in [5]. In addition, positioning the camera directly over the field of play would be difficult for exercises performed outdoors. Therefore, we propose a system that consists of a camera positioned atop a post and angled down at the field of play in such a way that the y axis of the field of play falls to the center of the camera image.

The video capture will be done with an Intel CS330 Web camera that has a 640x480 resolution with a 50 degrees diagonal a field of view and less than 5% distortion. Image capture is accomplished with the Java Media Framework and image processing and display is done with Java2 version 1.4.2. The GUI was designed to allow evaluation of captured images to determine object position accuracy.

6. CONVERTING PIXEL COORDINATES TO FLOOR POSITIONS

Figure 6 depicts the layout of the proposed camera system. The camera is located at the top of the triangle, height h above the floor. The y axis runs directly away from the camera and the camera's field of view (FOV), corresponding to the marked area in the lab, is shown as the shaded area.
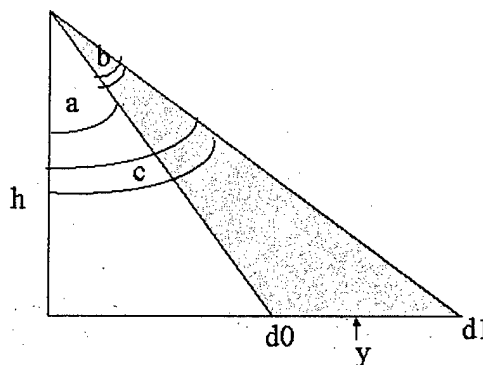

Figure 6. y axis of camera field of view

Point d0 indicates the closest point along the y axis that is in the FOV and d1 is the furthest point in the FOV. The pixels in the camera image that correspond to these points are denoted p0 and p1 respectively. Given physical measurements of h, d0 and d1 we can compute the three angles shown in the figure:

$$c = atan(d1(y)/h)$$

$$a = atan(d0(y)/h)$$

$$b = c - a$$

The pixels in the camera image have uniform angular spacing resulting in their physical size growing as they get further away from the camera position. The angular sector covered by each pixel is given by:

$$pixInc = b/\# pixels$$

Where # pixels is the pixel height of the camera image within the FOV. Given the information above we can then compute the physical y position of a pixel in the image using:

$$y = tan(a + (pix(y)-p0(y)) * pixInc) * h$$

for pixels beyond p0(y), where pix(y) is the pixel's y position in the image.

7. CAMERA POSITION TEST

The camera was placed on top of a coat rack post positioned along the center-line of the grid on the lab floor. The camera was then angled down and adjusted horizontally until the image was level. Further adjustments were done so that the y axis of the lab floor grid was vertical and near the center of the image snapshot inside the Java GUI. The resolution of the camera was set to its highest resolution which meant aligning the y axis as close to the 320th column of pixels as possible. Once positioned and adjusted, the height of the camera lens from the floor was 183cm.
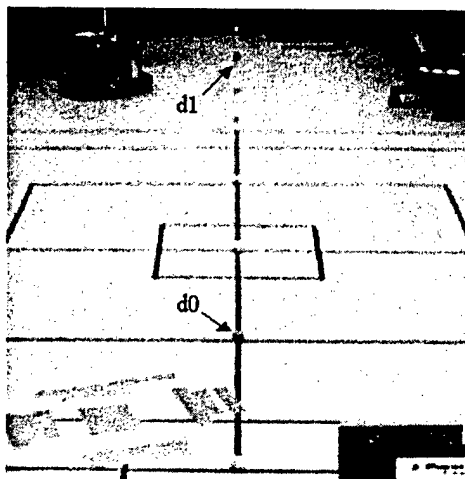

Figure 7. Close up of position markers

Next, a set of 8 brightly colored ping pong balls were placed 91.4cm apart along the y axis starting at a point 365.8cm away from the camera base as shown in the close up in figure 7. The green ball is at position d0 and the blue ball is at position d1.

Position d0 is 457.2cm from the camera base and d1 is 914.2cm away. This setup left one ball above and one below the measured range used in order to see how well the system would handle outside points.

The GUI shown in figure 8 was used to record the pixel coordinates within the camera image that correspond to d0 and d1 and to enter their respective measured ranges to the camera base. The measured height of the camera was also entered.
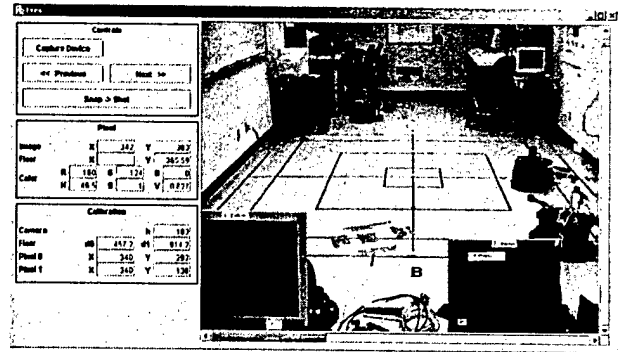

Figure 8. Image Evaluation GUI

The GUI then displayed pixel coordinates along with the measured y axis displacement from the camera base for each pixel as the mouse pointer was moved around the image. To find the calculated position of each ball, the mouse pointer was positioned as close to the bottom most point on each ball. The coordinates and y distance reported by the program were recorded for each of the 8 balls. Based on the equipment setup in the lab the values for the remaining variables in figure 6 are:

a = 68.19°
b = 10.49°
c = 78.68°
pixInc = .06724°
p0(y) = 292
p1(y) = 136

Table 1 shows the marker positions computed based upon pixel location and the corresponding measured positions.

Table 1 – Marker Positions

Pixel Coord.	Computed (cm)	Measured (cm)	diff
320, 363	365.6	365.8	0.2
320, 292	457.2	457.2	0
320, 242	548.5	548.6	0.1
320, 205	639.8	640.0	0.2
320, 176	729.8	731.4	0.6
320, 154	823.3	822.8	0.5
320, 136	914.2	914.2	0
320, 122	999.3	1005.6	6.3

The average error between computed and measured positions for all markers was 1.11cm. The tests reveal that an average accuracy of 0.1% can be maintained for a linear distance of approximately 7.5 meters for this camera height and angle. Since the error appears to grow rapidly further away from the camera as shown by the measurement for the pixel at location x=320 and y=122, the most accurate linear distance for this image is from the pixel nearest the camera to the pixel for the furthest marker. Based on the initial dataset, pixel growth rate due to lens distortion is negligible for the y axis of this camera and are more related to camera angle and height. Additional testing with a larger dataset would be more conclusive.

Several factors are considered that will affect the error observed. Each pixel represents an area on the floor instead of an exact point. This means that the object in question is located somewhere within the area represented by the pixel. Due to the angular nature of the camera setup, putting the camera higher will reduce the pixel growth rate and increase accuracy. Image processing techniques that have difficulty choosing the best pixel to represent the center of an object will also introduce error. Being able to determine the mapping of physical points to pixels in an image provides an accurate method for determining position.

8. CONCLUSION

Testing shows that dead reckoning alone is not accurate enough to provide quantifiable results for experiments done in the lab. An absolute positioning system is needed and the proposed camera setup shows great potential. Test results show that the camera based approach shows much higher accuracy than dead reckoning. The ease of setting up this system will work well in the lab and outdoors where the camera can be positioned and calibrated with minimal effort.

9. FUTURE WORK

Further work to determine accuracy within the full FOV including the x direction is necessary to validate this system. The absolute positioning system that uses this information will operate by processing an image each second. A uniquely colored ball for each robot would provide a way to locate each robot. Techniques to automatically detect the ball and calculate it's center pixel are to be developed. Work will also be done to develop the communications necessary to transmit the updated position to the lead robot once it's new position has been determined.

10. ACKNOWLEDGMENTS

11. REFERENCES

[1] James Kinsey and Louis Whitcomb, 'Preliminary Experiments with a Calibration Technique for Gyro and Doppler Navigation Sensors for Precision Underwater Navigation', Proceedings of the 13th Intl. Symposium on Unmanned Untethered Submersible Technology, August 2003, Durham, NH

[2] Kilfoyle, D.B. and Baggeroer, A. B., 'The State of Art in Underwater Acoustic Telemetry', IEEE Journal of Oceanic Engineering', vol. 25, no. 1 Jan 2000

[3] 'Pioneer 2 / PeopleBot Operations Manual', ActivMedia Robotics, LLC., Copyright © September 2002

[4] M. Arbatzat, S. Freitag, M. Fricke, R. Hafner, C. Heermann, K. Hegelich, A., Krause, J. Kr"uger, M. Lauer, M. Lewandowski, A. Merke, H. Muller, M. Riedmiller, J. Schanko, M. Schulte-Hobein, M. Theile, S. Welker, D. Withopf, 'Creating a Robot Soccer Team from Scratch: the Brainstormers Tribots', Universit" at Dortmund, Lehrstuhl Informatik I, 44221 Dortmund, Germany

[5] Janez Pers, Stanislav Kovacic, 'Nonparametric, Model-Based Radial Lens Distortion Correction Using Tilted Camera Assumption', University of Ljubljana, Tr" za"ska 25, SI-1000 Slovenia